Journal of Electron Microscopy **52(2)**: 119–124 (2003)

Full-length paper

Analytical TEM observation of Au and Ir deposited on rutile TiO_2

Tomoki Akita[1,*], Mitsutaka Okumura[1], Koji Tanaka[1], Susumu Tsubota[1] and Masatake Haruta[2]

National Institute of Advanced Industrial Science and Technology, [1]Special Division for Green Life Technology, 1-8-31 Midorigaoka, Ikeda, Osaka 563-8577 and [2]Research Institute for Green Technology, 16-1 Onogawa, Tsukuba, Ibaraki 035-8569, Japan

[*]To whom correspondence should be addressed. E-mail: t-akita@aist.go.jp

Abstract As a model catalyst, gold and iridium were co-deposited on a single crystal of rutile TiO_2 using the deposition precipitation method in order to clarify the synergetic effect of the combination of Au with Ir on the catalytic performance of the oxidative decomposition of odour and dioxins. Analyses by means of high-resolution transmission electron microscopy, energy-dispersive X-ray spectroscopy and electron energy-loss spectroscopy revealed that pillars of IrO_2 grew on the TiO_2 substrate to each of which one Au nanoparticle was attached. This mushroom-like structure appeared to be formed by self-organization of Au, Ir and oxygen. Epitaxial contact was observed between the Au nanoparticle/IrO_2 pillar and IrO_2 pillar/TiO_2 substrate interfaces. The growth process of the structure was investigated by transmission electron microscope observations of the Au-Ir complex before and after heating in air.

Keywords Au, Ir, TEM, deposition precipitation, nanoparticle, self-organization

Received 6 November 2002, accepted 30 January 2003

Introduction

Recently we have found that Au catalyst in combination with Ir shows high catalytic activity for the decomposition of dioxins at temperatures below 473 K. Although Ir alone was poorly active for the decomposition of orthochlorophenol, a substitute for dioxins in catalytic tests, it could appreciably boost the catalytic activity of Au [1]. However, Ir is rarely used alone as a catalyst in industry since it is scarce and expensive. Hence, it is often used as an additive to other metal catalysts, for example the Ni-Ir catalyst used for partial oxidation of methane to synthesis gas [2], the Pt-Ir-Rh catalyst used for nitrogen oxide decomposition in exhaust gases [3] and the Pt-Ir catalyst used for reforming catalyst in the petroleum industry [4]. Bimetallic or multicomponent catalysts usually have complicated structures [1]. It is quite difficult to clarify the effective structure as a catalyst, since they are often supported separately on the support surface or they form an alloy phase. The surface alloy has the possibility to change catalytic property, since it changes the adsorption energy of reaction molecules by the ligand effect [5]. Furthermore, it has also been found that the bimetallic particles form an ordered structure, such as the core-shell type [6,7]. Thus, a complex consisting of just two elements can form various structures depending on the components and synthesis process. Hence, it is worthwhile and indispensable to reveal the structure of the metal complex of nanoparticles at the atomic level in order to design and develop new functional catalysts that have well-ordered structures under nanoscale or atomic scale control. The catalytic properties should be influenced by the surface structure of the bimetallic particles and the contact structure with the support surface. The result would be the possibility of developing multifunctional catalysts by controlling the structure of the component catalysts at the nanoscale.

In this work, Au and Ir were simultaneously deposited on a TiO_2 single crystal using the deposition precipitation (DP) method [8], as a model structure of Au-Ir bimetallic catalyst. Observations were made by means of analytical transmission electron microscopy (TEM) using energy-dispersive X-ray spectroscopy (EDS) and electron energy-loss spectroscopy (EELS). The combination of Au and TiO_2 is interesting since it shows an obvious synergy effect for low temperature CO oxidation [8]. Studying the effect of adding Ir particles to pro-

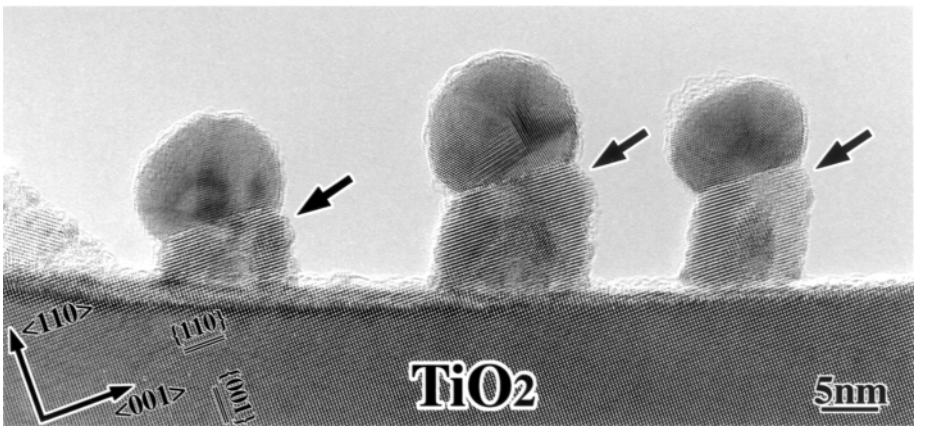

Fig. 1 A TEM image of Au-Ir deposited on a TiO_2 single crystal prepared using the DP method with calcination at 673 K for 4 h in air.

duce a catalyst for the decomposition of dioxins, as mentioned above, was considered to be of further interest. It is important to prepare the model structure utilizing as closely as possible the method to be used for the preparation of real catalysts, in order that techniques learned can be applied to the development of the new catalyst. This also makes it possible to discuss the catalytic activity and structure of the catalyst in detail.

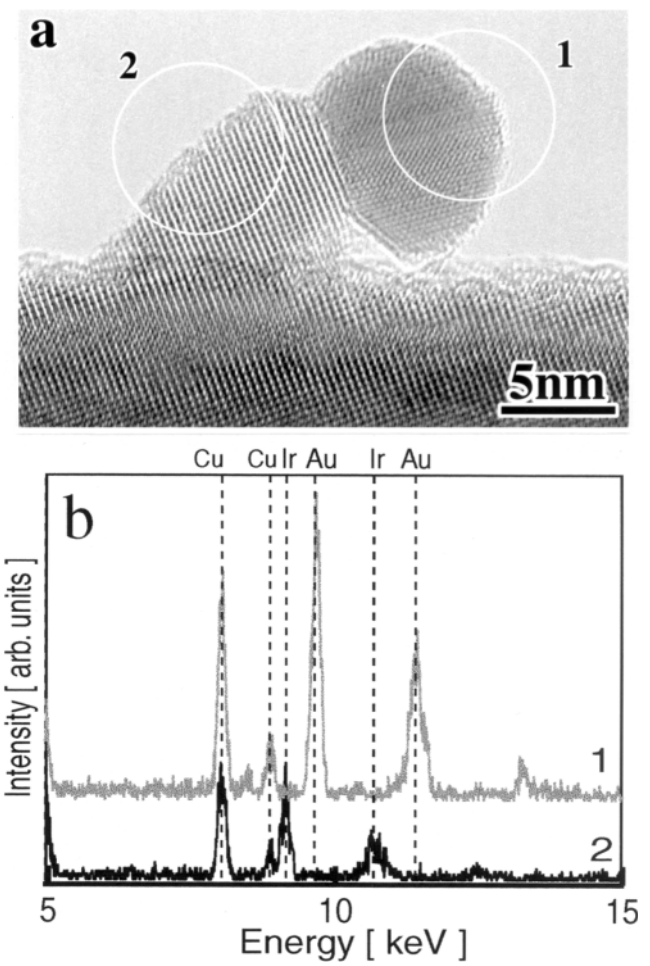

Fig. 2 A TEM image of Au-Ir deposited on TiO_2 (a) and corresponding EDS spectra obtained from each area indicated in the TEM image (b).

Methods

Using the DP method [8] that is usually employed to prepare highly dispersed gold particles on metal oxide supports, Au and Ir were simultaneously deposited on a rutile TiO_2 single crystal at an atomic ratio of 5 : 2. A 0.25–0.4 mm thick single crystal wafer of TiO_2 commercially produced by Earth Chemical Co., Japan was crushed in air and a cleaved fragment ($\sim 0.4 \times 1.5 \times 0.5$ mm^3) was used as a substrate. It was straightforward to determine the crystal orientation by optical microscopy and the cleaved face was found to be $TiO_2\{110\}$. One-hundred-ml solutions of $HAuCl_4$ (1×10^{-3} mol l^{-1}) and $IrCl_4$ (4×10^{-4} mol l^{-1}) were heated to 343 K and the pH of each solution adjusted to between 7 and 8 by independently adding NaOH solution. The two solutions were then mixed and the fragments of TiO_2 single crystal soaked in the resulting solution and aged for 1 h. The fragments were then washed with distilled water several times in order to remove residual sodium and chloride ions. After vacuum drying at 0.4 Pa for 15 h, the Au-Ir/TiO_2 sample was heated in air at 573–773 K for 4 h.

The fragment of Au-Ir/TiO_2 was fixed on a single-hole 3 mm Cu or Mo disc and this assembly set in the double-tilt sample holder of the TEM. The thin part of the edge of the TiO_2 fragment was observed by TEM. Observations were performed using a JEOL JEM-3000F TEM at an accelerating voltage of 300 kV. The compositions were EDS analysed using a Noran Vantage EDS system. The EELS measurements were performed using a Gatan imaging filter with a DigiScan scanning transmission electron microscope (STEM) digital control system.

Results and discussion

Figure 1 shows a typical TEM image of the Au-Ir deposited on a TiO_2 substrate after heating in air at 673 K. The incident electron was parallel to the rutile TiO_2<110> direction, and lattice fringes of 0.33 nm and 0.29 nm, corresponding to $TiO_2\{110\}$

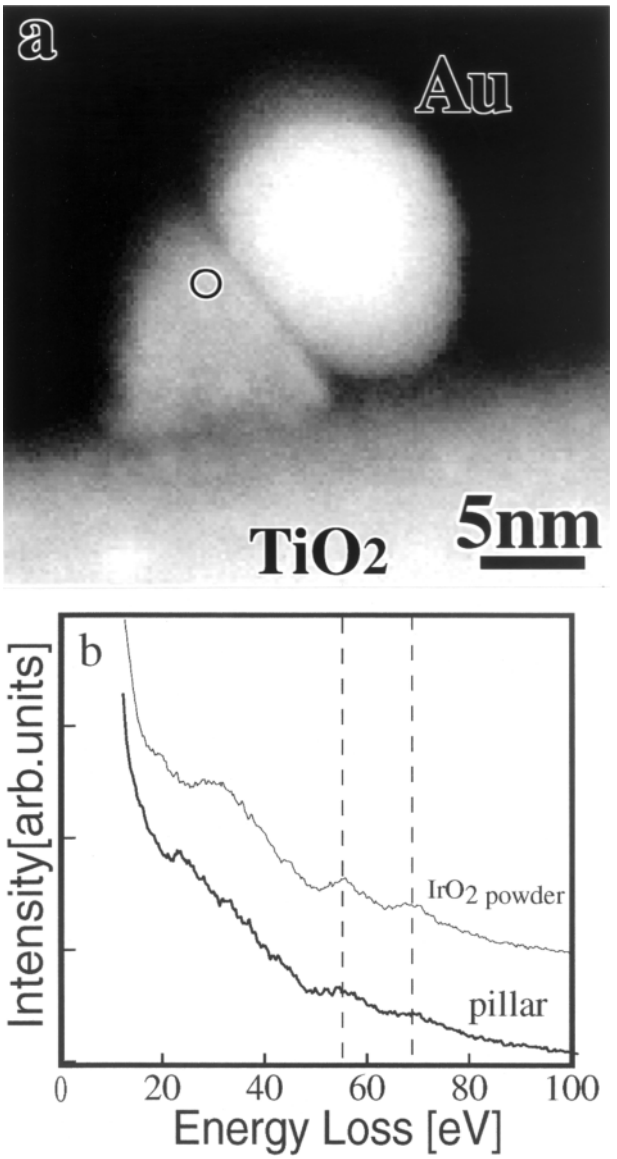

Fig. 3 An ADF-STEM image of Au-Ir deposited on TiO_2 (a) and EELS spectra obtained from the point indicated in the ADF-STEM image and standard sample of IrO_2 powder (b).

and TiO_2{001}, respectively, were clearly observed. The remarkable feature of this Au-Ir/TiO_2 structure was that a self-organized mushroom shape was formed consisting of a metal particle sitting on a pillar of ~10 nm width and 5–10 nm height, as indicated by arrows. Metal particles of ~5–10 nm were seen as dark contrast. Some had defects, such as twinning. The interfaces between metal particle and pillar were sharp and composed of a specific crystal plane.

Figure 2 shows a TEM image of the Au-Ir/TiO_2 and EDS spectra obtained from each area indicated in the TEM image. The interfaces between metal particle and pillar are as sharp in this image as those seen in Fig. 1. From the metallic particle placed on the top of the pillar, indicated by circle 1, X-ray signals of Au-L_α and L_β lines were observed at ~9.7 and 11.4 keV, but X-ray signals from the Ir were not. From the pillar, indicated by circle 2, Ir-L_α and L_β lines were observed at 9.2 and 10.7 keV, but X-ray signals from the Au were not. The Cu peaks seen at ~8.8 and 8.0 keV appeared as background noise from the Cu disc supporting the sample. This confirmed that the Au was separately deposited as a metallic particle on the pillar without forming an alloy with the Ir.

Figure 3 shows an annular dark-field STEM (ADF-STEM) image of the Au-Ir/TiO_2 and EELS spectra of the low-loss region obtained from the point indicated in the ADF-STEM image, and a standard sample of IrO_2 powder (purity >99.5%; High Purity Chemicals, Japan). Gold particles can be seen as bright, strongly contrasted areas in the ADF-STEM images. From the point in the pillar indicated in the ADF-STEM image, small peaks corresponding to IrO_2 [9] were observed at 54 and 68 eV. However, there were no peaks at ~48 eV, which would correspond to TiO_2. The EELS spectrum shape obtained from the pillar was the same as the standard spectrum measured from IrO_2 powder. The pillar had a crystalline structure and epitaxial growth on the TiO_2 substrate, as shown in the HRTEM image of Fig. 4. Based on the measurements of lattice fringes from the HRTEM image together with EDS and EELS analyses, it was concluded that the pillar is composed of IrO_2. The crystal structure of IrO_2 is a rutile structure and its lattice constant ($a = b = 0.450$ nm, $c = 0.315$ nm) is close to that of rutile TiO_2 crystal ($a = b = 0.459$ nm, $c = 0.296$ nm). The lattice mismatch was 2% for TiO_2{110} at 0.325 nm and IrO_2{110} at 0.318 nm, and 6% for TiO_2{001} at 0.296 nm and IrO_2{001} at 0.315 nm. Although the lattice mismatch of (001) was slightly large, the IrO_2 pillar did grow on the rutile TiO_2 substrate with the epitaxial relationship of TiO_2 <110>,<001> // IrO_2 <110>, <001>. The interface between TiO_2 and IrO_2 was not composed of a specific low index crystal plane. The pillars grew on the vicinal surfaces of the TiO_2 substrate, as can be observed in Figs 1, 2 and 4.

It is difficult to distinguish interfaces using the TEM images, but locations can be roughly estimated from the intensity of the ADF-STEM images since the intensity of IrO_2 is stronger than that of TiO_2. The interface was formed approximately at the crystal plane of the original TiO_2 surface that does not have a low index plane. The interface between the Au particle and IrO_2 pillar was formed precisely at IrO_2{110} and Au{100}. The growth direction of the pillar was approximately at IrO_2<110> and TiO_2<110>. It was observed that in some instances pillars grew in the TiO_2{001} direction, and in these cases the interface of Au and IrO_2 was not sharp compared with the pillars growing at TiO_2<110>. These pillars were composed of IrO_2 crystal, but the structure seemed to be incomplete, as indicated by the contrast of the TEM image not being homogeneous. It was often observed that the centre part of the pillars showed weak contrast. This feature was obvious in the ADF-STEM images that are sensitive to the thickness of the sample. It seemed that these pillars were hollow in structure. Such a feature could be related to the formation mechanism of the pillar structure, the details of which are under consideration.

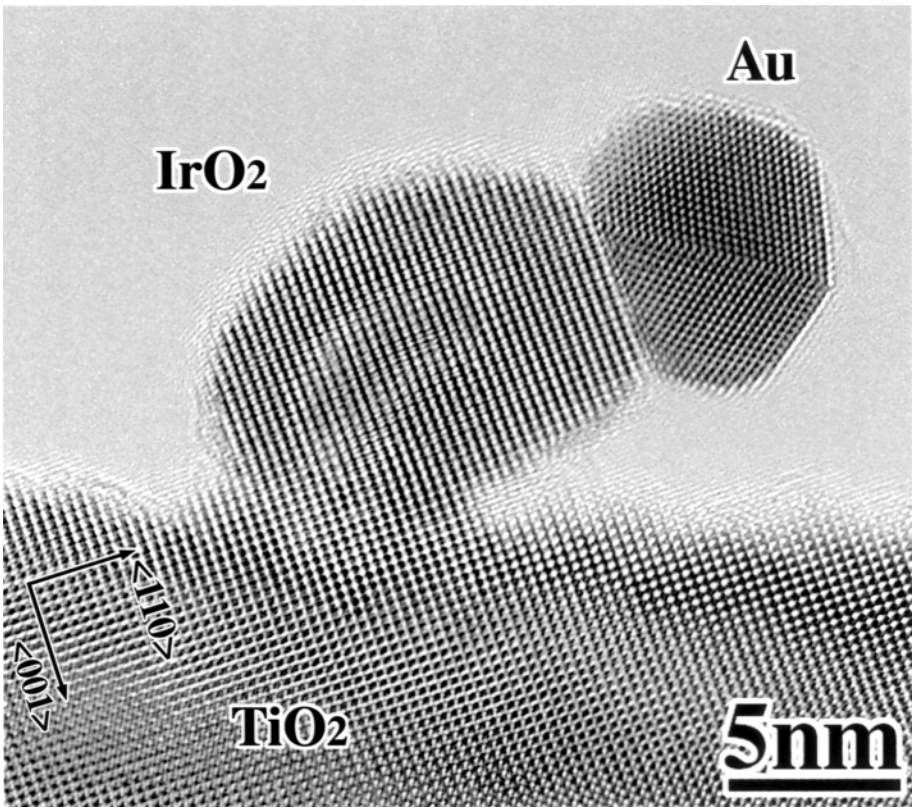

Fig. 4 A HRTEM image of Au-Ir deposited on TiO_2.

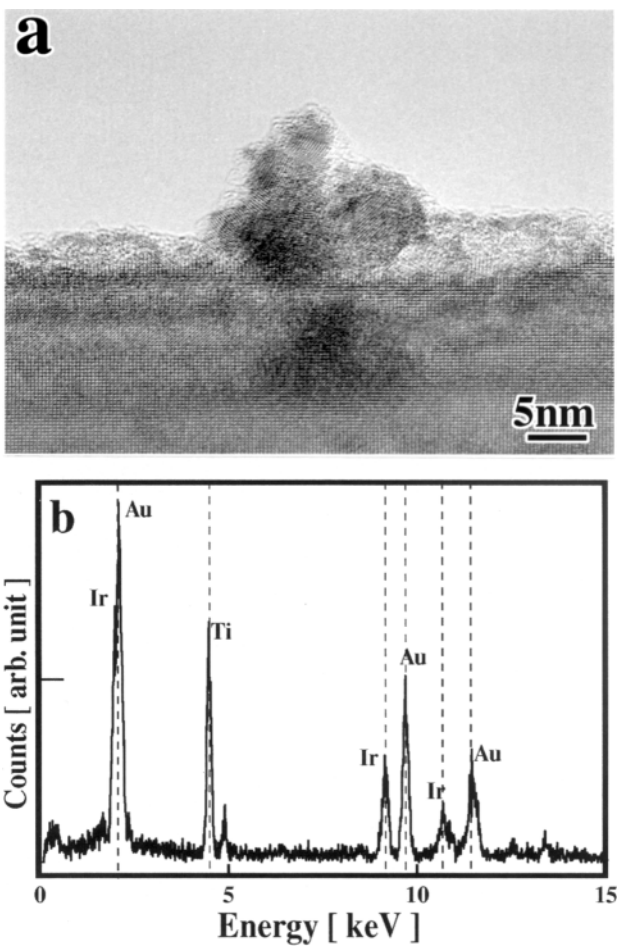

Fig. 5 A TEM image of Au-Ir deposited on TiO_2 before calcination (a) and EDS spectrum obtained from the particle (b).

In order to study the growth mechanism of the IrO_2 pillar structure, an Au-Ir/TiO_2 sample was observed before heating. Figure 5a shows the TEM image of Au-Ir deposited on TiO_2 after vacuum drying and before heating. Polycrystalline-like particles were observed on the TiO_2 surface, but no pillar structures were seen at all. It would seem that the particles were formed by the mixture of hydroxide of Au and Ir [8]. Particles show partially weak contrast similar to the amorphous phase and lattice fringes of metals. The EDS spectrum obtained from a particle is shown in Fig. 5b. The peaks from the Au and Ir were clearly observed and it was thereby confirmed that the Au-Ir complex was deposited on the TiO_2 surface by DP.

Figure 6 shows TEM images of a particular Au-Ir/TiO_2 sample taken from the same position before (Fig. 6a) and after heating in air at 773 K for 4 h (Fig. 6b). It was successfully confirmed that an IrO_2 pillar grew from the complex particles during the heating process in air. The Au particles contained defects and the IrO_2 pillar formed an incomplete crystal. However, the IrO_2 pillar was well crystallized near the TiO_2 substrate. This shows that the TiO_2 substrate affected the growth process of the crystalline pillar. It is not feasible that the small Ir clusters diffused on the TiO_2 surface and formed IrO_2 pillars, since iridium clusters were observed on the TiO_2 surface around IrO_2 pillars even after calcination at 773 K.

From the above observations the growing process of the IrO_2 pillar can be schematically drawn (Fig. 7). Au-Ir complexes

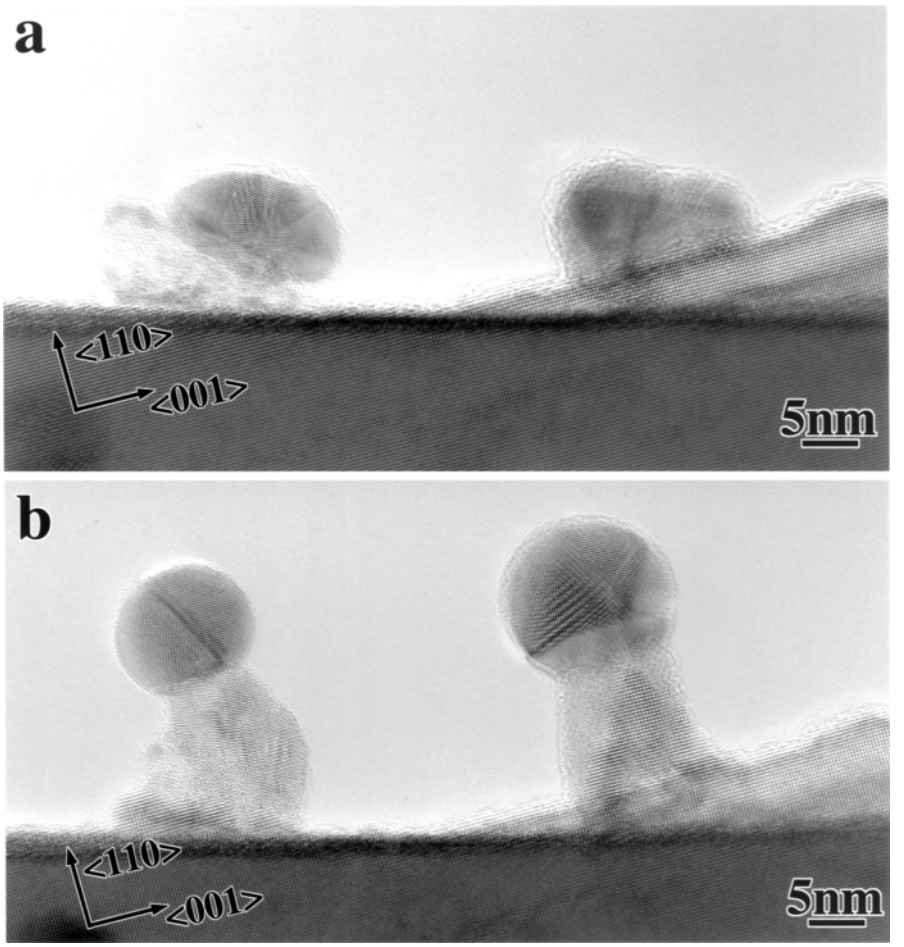

Fig. 6 Transmission electron microscopy images of Au-Ir deposited on TiO_2 before calcination (a) and after calcination (b).

containing Au hydroxide and Ir hydroxide were deposited on the TiO_2 surface during aging in the aqueous solution. Iridium dioxide was formed at the interface between the Au-Ir complex and TiO_2 substrate during calcination in air. This is feasible since it is known that iridium forms an oxide when heated at 573–773 K in air [10]. During calcination, Au atoms were aggregating and IrO_2 crystals forming while residual iridium atoms were being oxidized. Once the Ir was completely oxidized, the Au particles were left on the top of the IrO_2 pillars. It is interesting to note that the crystalline IrO_2 was formed from this Au-Ir structure while Ir tended to form amorphous iridium oxide when Ir without Au particles was deposited on TiO_2 using the DP method. Gold particles seem to act as a 'catalyst' promoting the crystallization of the IrO_2. Vapour–liquid–solid growth [11] is well known as a mechanism for growing semiconductor whiskers or nanowires using metal particles as a catalyst [12–14]. In the preparation process of the Au-Ir/TiO_2 structure shown here, it is not likely that iridium or iridium oxide vapour were supplied to the Au particles during the heating process at 573–773 K. In the present case, the growth of the IrO_2 pillars might be limited by the initial amount of iridium included in the Au-Ir complex particles.

The unique structure described above was observed when a rutile single crystal of TiO_2 was used as a substrate. However, it is not clear whether a similar structure could be formed if the same method was used with a powdered TiO_2 support having a large surface area. Hence, no conclusive remarks can be made concerning the relationship between catalytic activity and the structure of the Au-Ir complex at the present stage of research. Nevertheless, it is likely that this Au-Ir complex structure forming an interface between Au and metal oxide support will appreciably affect the catalytic activity of the Au/TiO_2 catalyst. Our future work concerning the relationship between the structure and the catalytic activity will include further discussion on this important issue. It is anticipated

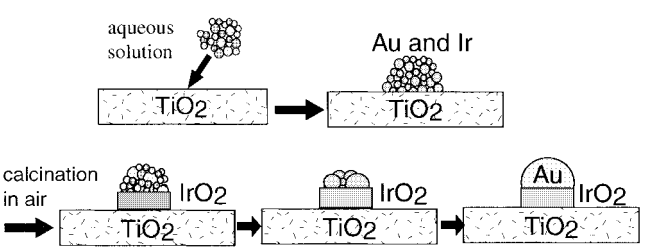

Fig. 7 Schematic drawing of the growth model of Au particle–IrO_2 pillar structure on TiO_2.

that these self-organized structures can be employed to create new ordered structure catalysts under nanoscale control.

Concluding remarks

A gold and iridium complex was formed on a rutile TiO_2 single crystal using the DP method usually employed to prepare Au supported catalysts. Analytical TEM observation using EDS and EELS revealed the following facts.

(i) The Au particles and IrO_2 formed self-organized ordered structures in which Au particles were placed on the top of IrO_2 pillars formed on the TiO_2 substrate.

(ii) The pillars of IrO_2 grew on the TiO_2 substrate by the epitaxial relation of TiO_2<110>, <001> // IrO_2<110>, <001>.

(iii) The crystalline IrO_2 pillars were formed from an Au-Ir complex by oxidation of Ir during a heating process in air.

Acknowledgements

This study was supported by a research grant from the New Energy and Industrial Technology Development Organization (NEDO project ID: 00A38006b).

References

1 Okumura M, Akita T, Haruta M, Wang X, Kajikawa O, and Okada O (2003) Multi component noble metal catalysts prepared by sequential deposition precipitation for low temperature decomposition of dioxin. *Appl. Catal. B: Environmental* **41**: 43–52.

2 Nakagawa K, Ikenaga N, Teng Y, Kobayashi T, and Suzuki T (1999) Partial oxidation of methane to synthesis gas over iridium-nickel bimetallic catalysts. *Appl. Catal. A: Gen.* **180**: 183–193.

3 Komatsu K (1997) A new type of three-way catalyst for lean burn gasoline engine. *Shyokubai* **39**: 216–221.

4 Sinfelt J H and Via G H (1979) Dispersion and structure of platinum-iridium catalyst. *J. Catal.* **56**: 1–11.

5 Srnova-Sloufova I, Lednicy F, Gemperle A, and Gemperlova J (2000) Core-Shell(Ag)Au bimetallic nanoparticles: analysis of transmission electron microscopy images. *Langmuir* **16**: 9928–9935.

6 Tada H, Suzuki F, Ito S, Kawahara T, Akita T, Tanaka K, and Kobayashi H (2002) Adsorption of 2,2′-dipyridyl disulfide on Au/Pt Core/Shell bimetallic clusters loaded on TiO_2: fine control of adsorptivity for organosulfur compounds. *Chem. Phys. Chem.* **7**: 617–620.

7 Gauthier Y, Schmid M, Padovani S, Lundgren E, Bus V, Kresse G, Redinger J, and Varga P (2001) Adsorption sites and ligand effect for CO on an alloy surface: a direct view. *Phys. Rev. Lett.* **87**: 036103.

8 Tsubota S, Cunningham D A H, Bando Y, and Haruta M (1995) Preparation of nanometer gold strongly interacted with TiO_2 and the structure sensitive in low-temperature oxidation of CO. In: *Preparation of Catalysts IV*, eds Poncelt G *et al*., pp. 227–234 (Elsevier, Amsterdam).

9 Ahn C C and Krivanek O L (1983) *EELS Atlas.* (Gatan).

10 Wang T and Schmidt L D (1980) Morphology and redispersion of Ir on SiO_2 in oxidizing and reducing atmospheres. *J. Catal.* **66**: 301–315.

11 Wagner R S and Ellis W C (1964) Vapor–liquid–solid mechanism of single crystal growth. *Appl. Phys. Lett.* **4**: 89–90.

12 Bootsma G A and Gassen H J (1971) A quantitative study on the growth of silicon whiskers from silane and germanium whiskers from germane. *J. Crystal Growth* **10**: 223–234.

13 Hiruma K, Murakoshi H, Yazawa M, and Katsuyama T (1996) Self organized growth of GaAs/InAs heterostructure nanocylinders by organometallic vapor phase epitaxy. *J. Crystal Growth* **163**: 226–231.

14 Ozaki N, Ohno Y, and Takeda S (1998) Silicon nanowhiskers grown on a hydrogen-terminated silicon {111} surface. *Appl. Phys. Lett.* **73**: 3700–3702.